Oscillatory signatures of crossmodal congruence effects: An EEG investigation employing a visual-tactile pattern matching paradigm

Florian Göschl[a⋆], Uwe Friese[a], Jonathan Daume[a], Peter König[a,b], and Andreas K. Engel[a]

[a] Department of Neurophysiology and Pathophysiology,

University Medical Center Hamburg-Eppendorf,

Martinistr. 52, 20246 Hamburg, Germany

[b] Institute of Cognitive Science, University of Osnabrück,

Albrechtstr. 28, 49069 Osnabrück

⋆ **Correspondence address:** Florian Göschl, Department of Neurophysiology and Pathophysiology, University Medical Center Hamburg-Eppendorf, Martinistr. 52, 20246 Hamburg, Germany.

E-mail: f.goeschl@uke.de

Abstract

Coherent percepts emerge from the accurate combination of inputs from the different sensory systems. There is ongoing debate about the neurophysiological implementation of crossmodal interactions in the brain, and it has been proposed that transient synchronization of neurons might be of central importance. Specifically, oscillatory activity in lower frequency ranges (< 30 Hz) has been implicated in mediating long-range communication as typically studied in multisensory research. In the current study, we recorded high-density electroencephalograms (EEG) while human participants were engaged in a visual-tactile pattern matching paradigm. Employing the same physical stimulation, separate tasks of the experiment either required the detection of predefined targets in visual and tactile modalities or the explicit evaluation of crossmodal stimulus congruence. Analysis of the behavioral data showed benefits for congruent visual-tactile stimulus combinations. Differences in oscillatory dynamics within the two tasks related to crossmodal congruence involved effects in the theta- (2-7 Hz), alpha- (8-13 Hz) and beta-band (13-25 Hz). Contrasting neuronal activity between the two tasks revealed differences in pre-stimulus alpha- and beta-band power, as well as differences in post-stimulus theta-band activity. Source reconstruction for these effects showed prominent involvement of superior temporal, parietal and prefrontal cortices – regions commonly implicated in multisensory integration. These results add to the increasing evidence that low frequency oscillations are well suited for studying integration in distributed brain networks, as demonstrated for crossmodal interactions in visual-tactile pattern matching in the current study. Additionally, neuronal activity at theta-, alpha- and beta-frequencies might subserve distinct processes relevant for multisensory integration, such as multisensory gating and crossmodal perceptual decision making.

Keywords: cortical oscillations, multisensory integration, visual-tactile, pattern matching, crossmodal congruence

1. Introduction

Multimodal processing and the integration of information from different sensory systems are crucial for adaptive behavior. Crossmodal interactions have been shown to impact perception (sometimes also resulting in illusory percepts, McGurk and McDonald, 1976) as well as a broad range of cognitive processes (Doermann and Naumer, 2005; Driver and Spence, 2000; Macaluso and Driver, 2005; Stein, 2012). Behavioral benefits resulting from the successful combination of inputs from different modalities are well documented, including improvements in target detection, discrimination or localization performance and faster response latencies (Diederich and Colonius, 2007; Forster et al., 2002; Frassinetti et al., 2002; Gillmeister and Eimer, 2007; McDonald et al., 2000; Molholm et al., 2004; Murray et al., 2001).

The question of how interactions between different sensory and other regions of the brain are implemented neurophysiologically remains a matter of dispute. Yet, it is evident that in order to quickly adapt to the environment fast changes of functional architecture of the brain network are essential (Jensen and Mazaheri, 2010). One mechanism that has been proposed to face the challenge of integration in distributed networks is transient synchronization of neurons (Singer and Gray, 1995; Engel et al., 2001; Varela et al., 2001; Womelsdorf et al., 2007). Only recently, synchronized oscillatory activity has also been linked to the integration of object features across sensory modalities (e.g. Lakatos et al., 2007; Kayser et al., 2008; for a review see Senkowski et al., 2008). Experimental support for a major role of neuronal oscillations in multisensory integration involves activity below 30 Hz in the theta-, alpha- and beta-bands (Doesburg et al., 2009; Gleiss and Kayser, 2014a; Hummel and Gerloff, 2005; Senkowski et al., 2006) as well as high frequency activity above 30 Hz (the gamma-band, see for example Bauer et al., 2009; Doesburg et al., 2008; Schneider et al., 2008; Schneider et al., 2011). Explicitly advocating different roles of high and low frequency activity in the

integration of distributed information, van Ackeren and colleagues (2014) have demonstrated for lexical-semantic stimulus material that linking modality-specific feature words to a target word is associated with enhanced gamma-band activity between 80 and 120 Hz, whereas integration of features from different modalities is mirrored in low-frequency power increases between 2 and 8 Hz. This matches results by von Stein et al. (2000) reporting synchronization in the gamma-band for monosynptically connected cortical areas and lower frequency synchronization for large-scale networks. Thus, Ackeren et al. (2014) position their findings within a framework proposed by Donner and Siegel (2011), arguing that low-frequency oscillatory activity is involved in the coordination of distributed neuronal populations, while local encoding happens within higher frequency ranges.

In order to study the multisensory interplay between vision and touch – a well-suited model for long-range communication in the brain – we employed a matching paradigm requiring the identification of concurrently presented visual and tactile dot patterns. In a behavioral study examining the interdependency of crossmodal stimulus congruence and attention (Göschl et al., 2014), we found that congruent as compared to incongruent visual-tactile stimulation reliably led to improved behavioral performance, mirrored in higher accuracies and shortened reaction times. In the present study, we used a similar paradigm and additionally recorded high-density electroencephalograms (EEG) to investigate the neurophysiological correlates of these congruence effects. Following the idea described earlier that integrative functions involving long-range interactions are predominantly mediated by lower frequencies (Donner and Siegel, 2011; von Stein et al. 2000; see also Hipp et al., 2011) we focused on oscillatory activity below 30 Hz in our analysis.

The visual-tactile matching paradigm used here involved two different tasks. In different blocks of the experiment, participants were either asked to (1) detect predefined target patterns that could appear in both sensory modalities (*detection task*) or, (2) explicitly evaluate the relationship between the two patterns and report whether they were the same or

not (*congruence evaluation task*). Keeping the physical stimulation exactly the same in both tasks, this design was highly suited determining inter-task differences associated with distinct cognitive demands of *detection* and *congruence evaluation* (including comparisons of pre-stimulus neuronal activity), as well as intra-task comparisons related to visual-tactile stimulus congruence. On the one hand, we expected modulations in preparatory neuronal activity related to task requirements, especially in alpha- and beta-frequencies (Mazaheri et al., 2014; van Ede et al., 2011; van Ede et al., 2014). On the other hand and in line with previous studies on crossmodal interactions and low frequency modulations (Barutchu et al., 2013; Doesburg et al., 2009; Gleiss and Kayser, 2014a; Gleiss and Kayser, 2014b; Hummel and Gerloff, 2005; van Ackeren et al., 2014; van Driel et al., 2014), we expected post-stimulus modulations in different frequency bands below 30 Hz, possibly reflecting different constituent factors of the complex process of multisensory integration. In order to further differentiate between subcomponents of visual-tactile interactions on a spatial scale, we reconstructed neuronal sources of frequency-band specific power using non-adaptive linear spatial filters (eLORETA).

2. Methods

2.1 Participants

Sixteen right-handed volunteers (12 female, mean age 25.4, range 21-33) were monetarily compensated for their participation in the study. All participants had normal or corrected to normal vision, and reported no history of neurological or psychiatric illness. The Ethics Committee of the Medical Association Hamburg approved the current study, and participants provided written informed consent prior to the recordings.

2.2 Task design

The experimental setup outlined in the following is similar to a previous behavioral study (Göschl et al., 2014), using only a subset of the visual-tactile matching paradigm described in detail ibidem (see Figure 1 for an overview of events and timing of the current experiment). Four spatial patterns, each of them formed by three dots, constituted the stimulus set (Figure 1A). Stimuli were presented visually on a computer monitor, appearing left of a central fixation cross, embedded in a noisy background. Concurrently, dot patterns were delivered haptically to participants' right index fingertip via a Braille stimulator (QuaeroSys Medical Devices, Schotten, Germany). Stimulus duration was 300 ms for both patterns.

Prior to the actual experiment, we conducted a delayed-match-to-sample training task to familiarize participants with the tactile patterns. In this training task, participants were asked to judge whether a sample stimulus (duration 300 ms) and a 1000 ms later on presented probe stimulus (also of 300 ms duration) were identical or not. Responses were given with the left hand via button press on a response box (Cedrus, RB-420 Model, San Pedro, USA) and visual feedback (a green '+' or a red '–') informed participants about the correctness of their response. After a minimum of five training blocks (each consisting of 16 trials) and a

matching performance of at least 80%, participants could proceed to the actual experiment. One participant not meeting this criterion was excluded after the training procedure.

The experimental session incorporated two different tasks (performed in separate blocks of the experiment), which both required the identification of concurrently presented visual and tactile patterns. In the *detection task*, participants were instructed to detect target stimuli that could appear in both modalities. In each experimental block, one out of the four dot patterns was defined as target (the other three patterns were non-targets, respectively) and introduced to the participants at the start of the block by simultaneously presenting it on the computer screen and by means of the Braille stimulator (four times). In the following experimental trials, targets could appear in the visual or the tactile modality alone, in both or in neither of the two. Participants had to decide whether the presented patterns matched the previously defined target stimulus or not and press one of two response buttons accordingly. In the *congruence evaluation task*, participants were asked to compare patterns across sensory modalities and report whether they were the same (congruent) or not. Again, responses were given via button press.

The timing was identical for the *detection* and the *congruence evaluation task* and is displayed in Figure 1B. The major difference compared to the experimental design realized in our earlier study is the wait interval of 1200 ms between stimulus presentation and response. This interval was chosen to prevent contamination of the EEG signal by activity resulting from response execution.

Each participant performed 1536 trials over two sessions recorded on separate days (with the two sessions happening within three days). The experimental design was counterbalanced in the presentation of congruent and incongruent stimulus pairs, target definitions and presentation frequencies of each of the four patterns across trials (for details see Göschl et al., 2014). We pooled data from the two recording sessions and grouped trials as follows: visual targets alone (a visual target appearing with a tactile non-target; labeled incongruent V in the

following), tactile targets alone (a tactile target presented with a visual non-target; incongruent T), and visual-tactile targets (congruent VT) as well as non-target congruent stimulus pairs and non-target incongruent pairs for the *detection task* (five conditions); for the *congruence evaluation task* we split trials in congruent and incongruent visual-tactile stimulus pairs, respectively. This procedure left us with a total of 192 trials for each condition (only the non-target incongruent pairs appeared 384 times to balance tactile and visual target trials). In the following, we focus on correctly detected (incongruent V, incongruent T and congruent VT) targets for the *detection task* and accurately identified congruent and incongruent stimulus pairs for the *congruence evaluation task*.

Key mapping (for 'target' and 'non-target'-, as well as 'congruent' and 'incongruent'-buttons) was counterbalanced across participants and sessions. To mask sounds associated with pin movement in the Braille cells, participants were presented with pink noise administered via foam-protected air tube earphones at 75 dB sound pressure level (Eartone, EAR Auditory Systems, AearoCompany). We used Presentation software (Neurobehavioral Systems, version 16.3) to control stimulus presentation and to record participants' response times (RT) and accuracies.

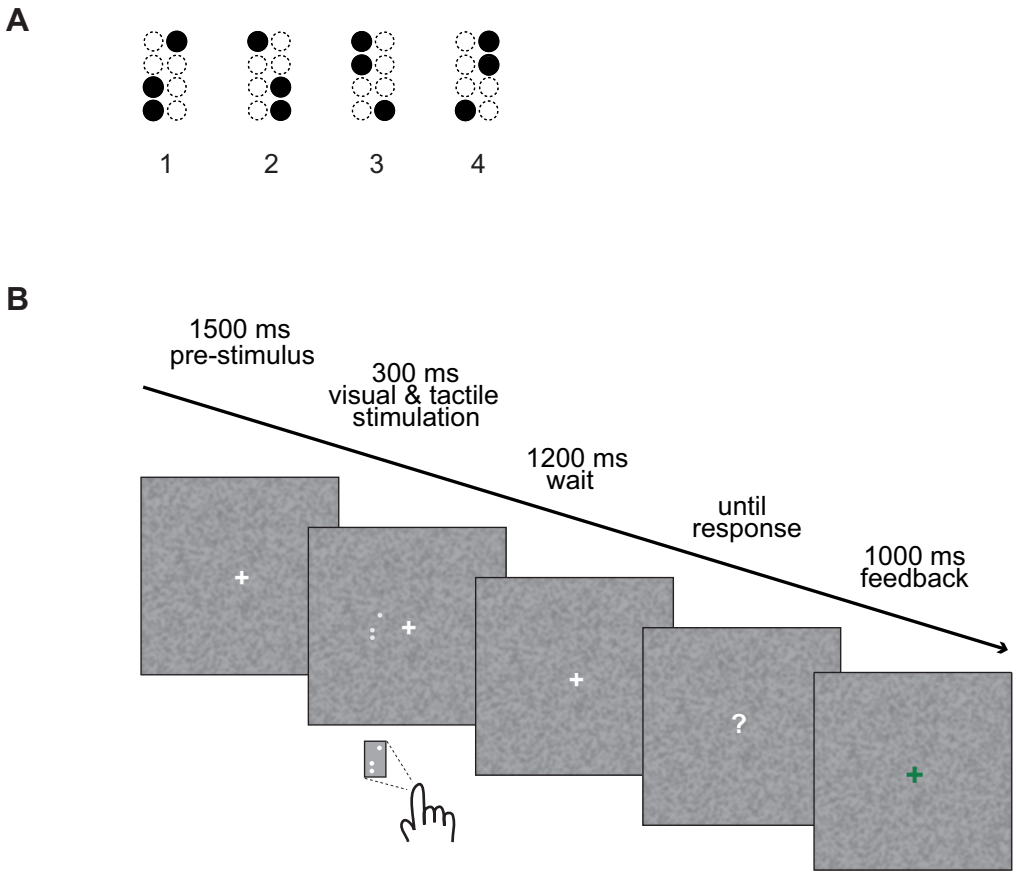

Figure 1. Schematic representation of the visual-tactile matching task. (**A)** The four pattern stimuli used in our experiment. (**B)** The trial sequence. After a pre-stimulus interval of 1500 ms, visual and tactile stimuli were presented simultaneously for 300 ms, followed by a wait interval of 1200 ms. After that, a question mark appeared on the screen indicating that responses could be given. After button press, every trial ended with visual feedback (1000 ms).

2.3 EEG recordings

EEG data were acquired from 126 scalp sites using Ag/AgCl ring electrodes mounted into an elastic cap (EASYCAP, Herrsching, Germany). Additionally, two electrodes were placed below the eyes to record the electrooculogram. EEG data were recorded with a passband of 0.016-250 Hz and digitized with a sampling rate of 1000 Hz using BrainAmp amplifiers (BrainProducts, Munich, Germany). The tip of the nose served as a reference during the recordings but subsequently we re-referenced the data to common average. Analysis of the EEG data was carried out in Matlab 8.0 (MathWorks, Natick, MA) using custom-made scripts, as well as routines incorporated in EEGLAB 11.0 (Delorme and Makeig, 2004;

http://sccn.ucsd.edu/eeglab/) and FieldTrip (Oostenveld et al., 2011; http://fieldtrip.fcdonders.nl). Offline, the data were band-pass filtered (0.3-180 Hz), downsampled to 500 Hz and epoched from – 400 to + 1400 ms around the onset of the simultaneously presented visual and tactile stimuli. All trials were inspected visually, and those containing EMG artifacts were rejected. Afterwards we applied an independent component analysis (ICA) approach to remove artifacts related to eyeblinks, horizontal eye movements and electrocardiographic activity. To control for miniature saccadic artifacts, we employed the COSTRAP algorithm (correction of saccade-related transient potentials; Hassler et al., 2011) that has been used to suppress ocular sources of high frequency signals (e.g. Friese et al., 2013; Hassler et al., 2013). With this multilevel artifact correction procedure, 88% of all recorded trials (range: 75% to 95%) were retained.

2.3.1 Spectral analysis

We derived time-frequency representations (TFRs) of the data via wavelet convolution in the frequency domain. Power spectra of the EEG signal were obtained from fast Fourier transforms and multiplied by the power spectrum of the complex Morlet wavelets [$\frac{e^{i2\pi tf}\, e^{-t^2}}{2\sigma^2}$; *t* represents time, *f* is frequency which increased in 30 logarithmic steps from 2 to 100 Hz, and σ defines the width of each frequency band, set according to $n/(2\pi f)$, where *n* stands for the number of wavelet cycles which increased from 3 to 10 in logarithmic steps (Cohen and Donner, 2013; Cohen, 2014)]. Then, the inverse fast Fourier transform was taken. All frequency transformations were done at the single-trial level before averaging. Power estimates for specific frequencies at each time point were defined as the squared magnitude of the complex convolution result $\{real[z(t)]^2 + imaginary[z(t)^2]\}$. To compute the relative signal change, power data were normalized with respect to a pre-stimulus baseline window. The

baseline power was calculated as the average from – 250 ms pre-stimulus to 0 (stimulus onset).

To obtain the induced, non-phase-locked part of the signal power, we computed the event-related potential (ERP) and subtracted it from the time domain signal on each trial (Kalcher and Pfurtscheller, 1995). This procedure was carried out for each condition, electrode and subject separately. Afterwards, the time-frequency decomposition was conducted as described in the previous paragraph. Analysis was done for both, total and induced power with results being highly comparable. For reasons of clarity, we focus on the analysis of induced power in the following.

Based on visual inspection of the baseline corrected TFR averaged across all sensors, experimental conditions (also including the non-target conditions for the *detection task*) and participants, we selected five time-frequency windows of interest. For the *detection* (Figure 2A) as well as the *congruence evaluation task* (Figure 2B), we defined two theta-band windows (2 to 7 Hz), an early one from 0 to 750 ms post-stimulus, and a late one from 750 to 1250 ms, an alpha-band (decrease) window (8 to 13 Hz) from 250 to 750 ms, a beta-band (decrease) window (13 to 25 Hz) from 250 to 750 ms and a second beta-band (rebound) window (13 to 25 Hz) from 750 to 1250 ms after pattern presentation. Within these time-frequency windows, we investigated stimulus-congruence related intra-task differences, separately for the *detection* and the *congruence evaluation task*. Activity at frequencies above 30 Hz was analyzed as well but did not show reliable modulation in response to visual-tactile stimulation.

To assess global differences in oscillatory dynamics related to different cognitive demands of the two tasks (inter-task differences), we compared neuronal activity directly preceding the presentation of the visual and tactile stimuli (in a time window from – 250 ms to 0) in alpha- and beta-frequencies. Additionally, we checked for task effects by comparing responses to congruent pairs of stimuli *between* the two tasks. Using the time-frequency windows

described above, we contrasted responses to congruent VT targets of the *detection task* and matching stimulus pairs of the *congruence evaluation task*, i.e. two conditions employing identical physical stimulation and both requiring a positive detection response.

For the statistical analysis of sensor level power data, we applied a cluster level randomization approach (Maris and Oostenveld, 2007) as implemented in FieldTrip (Oostenveld et al., 2011). This procedure has been used previously (see for example Jokisch and Jensen, 2007; Nieuwenhuis et al., 2008 and Mazaheri et al., 2014) and controls for Type I errors involving multiple comparisons (in our case over multiple sensors). First, data were averaged for the time and frequency window of interest and a t-statistic was computed for every sensor. Then, contiguous sensors falling below a p-value of 0.05 were grouped in clusters, with the sum of t-values in a given cluster being used in the cluster-level test statistics. Subsequently, the Monte Carlo estimate of the permutation p-value of the cluster was obtained by evaluating the cluster-level test statistic under the randomization null distribution assuming no condition difference. This distribution was created by randomly reassigning the data to the conditions across participants 1000 times and computing the maximum cluster-level test statistic. Analysis was carried out separately for all time-frequency windows defined in the preceding paragraph.

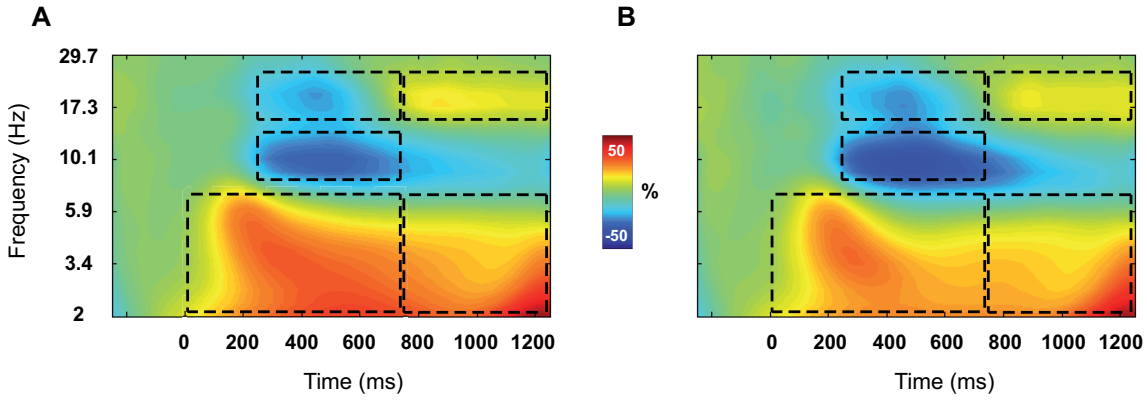

Figure 2. Grand average time-frequency representations (TFRs) for the two tasks. (**A**) TFR for the *detection task,* and (**B**) the *congruence evaluation task* with time-frequency windows of interest. Power data were averaged across all sensors, experimental conditions and subjects and are shown as % change to baseline.

2.3.2 Source estimation of frequency-specific activity

Neuronal sources of frequency-band specific activity were reconstructed using eLORETA (exact low-resolution brain electromagnetic tomography). eLORETA is a non-adaptive linear spatial filter with the property that single dipoles without additional noise can be localized exactly (for technical details see for example Pascual-Marqui, 2007). We calculated cross-spectral density (CSD) matrices between all 126 scalp EEG channels (excluding the EOG channels) in every frequency (2 to 100 Hz in 30 logarithmic steps) for six time windows of equal length. The time windows were: – 250 ms to 0, 0 to 250 ms, 250 to 500 ms, 500 to 750 ms, 750 to 1000 ms and 1000 to 1250 ms. Calculation of cross spectra was done separately for every participant and experimental condition in each trial. To derive the source estimates, we multiplied the real part of the frequency domain data (the real part of the cross spectrum) with the real-valued filter. We took the largest eigenvalue of the reduced 3 x 3 cross spectrum as a power estimate for each grid point. eLORETA computations were made in a realistic 3-shell head model based on the MNI152 template brain (Montreal Neurological Institute; http://www.mni.mcgill.ca). Source activity was estimated within a continuous grid of 3000 voxels and leadfields were calculated as described in Nolte and Dassios (2005). Source data were baseline corrected as well, with respect to an interval from – 250 ms to 0 (corresponding to the first time window of our CSD matrix calculation).

Across participants, paired t-tests were calculated analogous to the sensor level comparisons described above with the corresponding t-values being reported uncorrected. Anatomical labeling was done using the NFRI functions (Singh, Okamoto et al., 2005; http://www.jichi.ac.jp/brainlab/tools.html). MNI coordinates of maximal statistical differences at the source level are displayed in Table 2.

3. Results

3.1 Behavioral data

To determine whether behavioral performance within the *detection task* differed depending on visual-tactile stimulus congruence, we subjected accuracy and reaction time data for congruent VT, incongruent V and incongruent T targets to 1 x 3 repeated measures ANOVAs with Congruence as the within-subject factor. We found a significant effect of Congruence ($F_{1,\ 15}$ = 23.28, p < 0.01), with congruent VT targets being associated with the highest detection rate, followed by incongruent V targets and incongruent T targets (see Table 1 for mean accuracies of the different conditions). To further elucidate stimulus-congruence related effects, post hoc t-tests were conducted showing that congruent stimulation (VT targets) led to superior detection as compared to incongruent V targets (t_{15} = 4.37, p < 0.01) and incongruent T targets alone (t_{15} = 6.58, p < 0.01; paired sample t-tests). Mean reaction times (note that responses could only be given after a forced wait interval of 1200 ms after stimulus presentation) for the detection of congruent VT, incongruent V and incongruent T targets are also displayed in Table 1. Again, a repeated measures ANOVA revealed a significant effect of Congruence ($F_{1,\ 15}$ = 6.59, p < 0.01). Post hoc comparisons (paired sample t-tests) showed that reactions were fastest for the detection of congruent VT targets with a significant difference to incongruent T targets (t_{15} = 3. 11, p < 0.01) but only trended to significance for congruent VT targets and incongruent V targets (t_{15} = 1.91, p = 0.08). Thus, we did not observe a speed accuracy tradeoff; instead bimodal stimulation achieved consistently higher performance.

In order to compare behavioral performance on matching and non-matching visual-tactile pairs of stimuli in the *congruence evaluation task*, we employed paired sample t-tests. Across subjects, congruent pattern combinations trended to be associated with higher accuracy (t_{15} = 2.07, p = 0.06; see Table 1 for mean accuracies and reaction times). This is compatible with a

response bias 'in doubt towards congruence'. The analogous comparison for reaction times yielded no significant result.

Global differences in behavioral performance between the *detection* and the *congruence evaluation task* were assessed by calculating mean accuracies and reaction times within the two tasks (including non-target conditions for the *detection task*) and contrasting values between them (paired sample t-tests, two-tailed). Behavioral metrics were comparable (no significant differences found). In addition, we analyzed performance on congruent VT targets of the *detection task* and matching pairs of the *congruence evaluation*. Contrasting these two conditions employing the same physical stimulation with different task demands, we found the former to be associated with significantly higher accuracies ($t_{15} = 5.42$, $p < 0.01$, paired sample t-test) and lower reaction times ($t_{15} = 2.33$, $p < 0.05$).

Table 1. Behavioral data of the visual-tactile matching paradigm. Mean accuracies (ACC, shown in percent) and response times (RT, shown in ms), with standard deviations (SD) for the *detection* and the *congruence evaluation task* as well as the comparison of the two tasks.

	ACC (SD)	**RT (SD)**
Detection task		
Congruent VT targets	96.2 (3.6)	376 (193)
Incongruent V targets	88.5 (9.2)	390 (194)
Incongruent T targets	71 (16.3)	411 (193)
Congruence evaluation task		
Matching stimulus pairs	87.5 (7.6)	406 (200)
Non-matching stimulus pairs	80.4 (16.3)	417 (195)
Comparison between detection (also including non-targets) and congruence evaluation task		
Detection	82.9 (7.3)	410 (203)
Congruence evaluation	83.9 (10.8)	412 (197)

3.2 EEG data

The following section on results of our EEG sensor and source level analysis is subdivided in three parts: (1) stimulus-congruence related effects in the *detection task*, (2) differences between matching and non-matching stimulus pairs in the *congruence evaluation task* and, (3) a comparison of the two tasks. MNI coordinates and uncorrected t-values of maximal source level differences are displayed in Table 2.

3.2.1 Detection task

To analyze frequency-specific differences related to crossmodal stimulus congruence in the *detection task*, we compared responses to congruent VT and incongruent V targets as well as congruent VT and incongruent T targets separately in our time-frequency windows of interest (see above). Additionally, we reconstructed sources of neuronal activity for the different conditions as well as the maxima of condition differences. In the following, only statistically significant comparisons between conditions are reported.

Alpha-band power between 250 and 750 ms after stimulus presentation was reduced compared to baseline for congruent VT, incongruent V and incongruent T target cases (see condition topographies in Figure 3A). Comparing responses between conditions using cluster-based randomization tests yielded significant stimulus congruence-related differences. Decreases in alpha-band power were more pronounced for congruent VT targets compared to incongruent V targets as well as incongruent T targets. Topographical distributions of these differences as displayed in Figure 3B and 3D show significant clusters in right central and left posterior scalp regions ($p < 0.05$ for both clusters, tested two-sided).

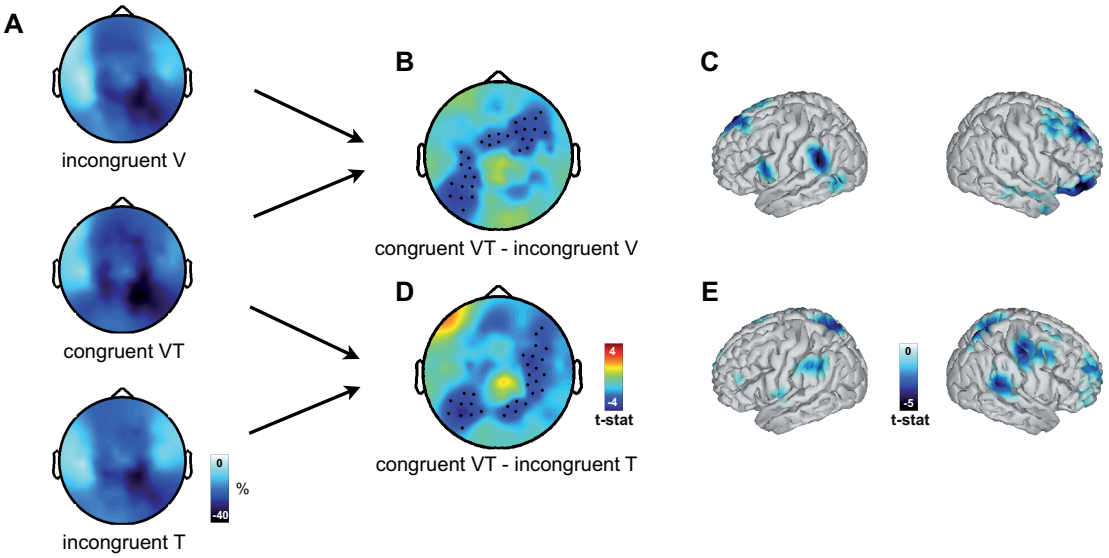

Figure 3. Comparison of alpha-band responses in the *detection task*. (**A)** Alpha-band power for frequencies between 8 and 13 Hz and a time window of 250 to 750 ms after stimulation plotted for the different conditions as relative change (%) to baseline. (**B**) Topography of the difference (shown in t-values) in alpha-band power between congruent VT and incongruent V target trials. A significant cluster ($p<0.05$) is apparent spanning from right central to left posterior scalp locations. (**C**) Statistical differences for the source level comparison of alpha-band responses between 250 and 750 ms in congruent VT and incongruent V target trials (tested two-sided with only negative, uncorrected t-values below the fifth percentile displayed here). For MNI coordinates of maxima see Table 2A. (**D-E**) Comparison of alpha-band responses on congruent VT and incongruent T trials. Presentation of results is analogous to the comparison in B-C. The cluster in (D) is significant with $p<0.05$.

Alpha-band power decreases across conditions between 250 and 750 ms after stimulation were maximal in right-hemispheric primary and secondary somatosensory cortices as well as premotor areas. Comparing responses to congruent VT and incongruent V targets revealed the strongest modulations to be located in prefrontal areas and left supramarginal gyrus (Figure 3C; see Table 2A for the respective MNI coordinates). Please note that statistical differences for all source level analyses are displayed in uncorrected t-values. Maxima for differences between alpha-band decreases to congruent VT and incongruent T targets on the other hand were predominantly located to the right hemisphere and found in premotor areas, supramarginal gyrus, somatosensory association cortex and superior frontal gyrus (Figure 3E).

Beta-band power also decreased in the 250-750 ms time window (see Figure 2A), without showing differences between conditions. As can be seen in Figure 4A for the different target

cases, beta-band activity over left-hemispheric regions exceeded baseline level in an interval of 750 to 1250 ms after stimulation. Cluster statistics revealed differences between beta-band responses to congruent and incongruent visual-tactile stimulation. Figure 4B shows a cluster (not reaching significance, $p = 0.1$) located in right-hemispheric central-posterior scalp regions for the difference of congruent VT compared to incongruent V targets, and Figure 4D a significant, centrally distributed cluster ($p < 0.05$) for the comparison of congruent VT and incongruent T targets. Having a closer look at condition wise activity patterns of beta-frequencies in the time window 750-1250 ms, it becomes evident that the difference between congruent VT targets and incongruent T targets is due to differences in right-hemispheric power decreases between conditions as well as beta-band rebound phenomena that are restricted to left-hemispheric regions.

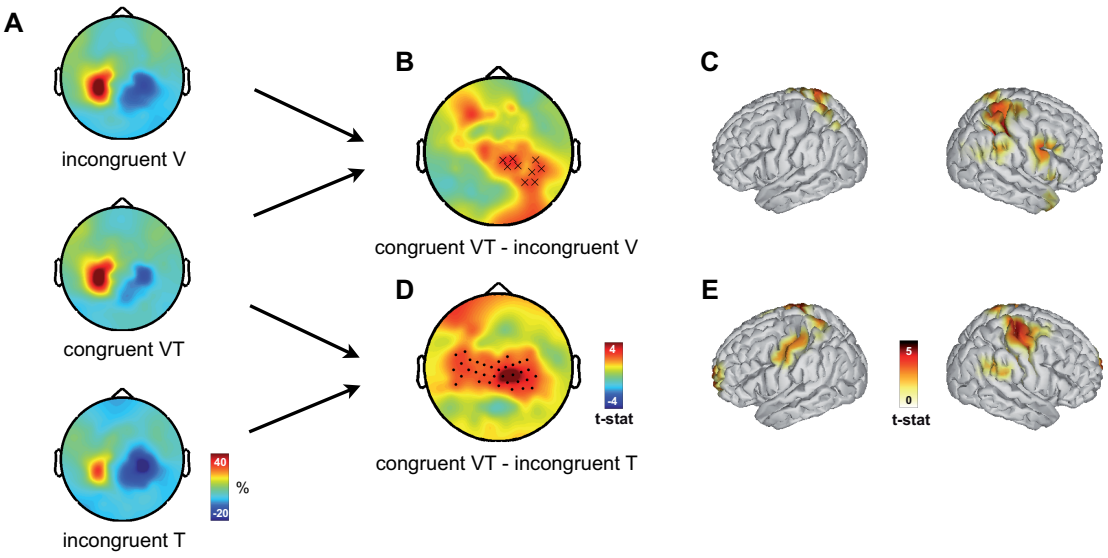

Figure 4. Comparison of beta-band responses in the *detection task*. (**A**) Beta-band power for frequencies between 13 and 25 Hz and a time window of 750 to 1250 ms after stimulation plotted for the different conditions as relative change (%) to baseline. (**B**) Topography of the difference (shown in t-values) in beta-band power between congruent VT and incongruent V targets in the same time window. A cluster (not reaching statistical significance, $p = 0.1$) in right central-posterior locations is apparent. (**C**) Statistical differences for the source level comparison of beta-band responses between 750 and 1250 ms in congruent VT and incongruent V target trials (tested two-sided with only positive, uncorrected t-values above the 95th percentile shown, see Table 2A for MNI coordinates). (**D-E**) Comparison of beta-band responses on congruent VT and incongruent T target trials. Presentation of results is analogous to B-C. The cluster in (D) is significant with $p<0.05$.

Beta-band increases between 750 and 1250 ms post-stimulus compared to baseline activity were limited to left-hemispheric areas and maximal in premotor cortex. Right-hemispheric decreases in the same time and frequency window also peaked in premotor areas. The strongest differences between congruent VT and incongruent V targets in the late beta-range were found in areas of right somatosensory association and premotor cortex (Figure 4C) with power decreases being more pronounced for incongruent V target cases. Differences for the comparison of congruent VT and incongruent T targets were located in prefrontal areas, right premotor cortex and left somatosensory and premotor cortices (Figure 4F).

3.2.2 Congruence evaluation task

Time-frequency windows were defined based on the grand average TFR (Figure 2B) in the same way as for the *detection task*. Only statistically significant comparisons between frequency-specific responses to matching and non-matching stimulus pairs in the *congruence evaluation task* and their corresponding source reconstructions are covered in the following.

Theta-band power at later processing stages (between 750 and 1250 ms after stimulation) was augmented compared to baseline at central scalp sites and locations overlying the temporal areas, whereas it was moderately reduced at right posterior sites (Figure 5A). Differences between congruent and incongruent pairs were mirrored in a significant positive cluster ($p < 0.05$) with broad right-hemispheric distribution (Figure 5B). Hence, congruent visual-tactile stimulus pairs were associated with higher theta-band power values.

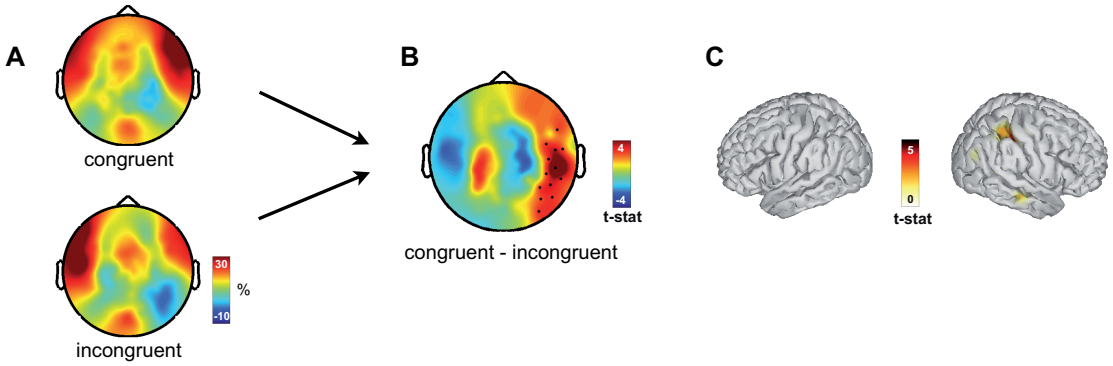

Figure 5. Comparison of theta-band responses in the *congruence evaluation task*. (**A**) Power for theta-frequencies (2-7 Hz) for congruent and incongruent stimulus pairs in a time window from 750 to 1250 ms after stimulation, expressed as relative change to baseline (in %). (**B**) Topography of the differences (shown in t-values) in late theta-band power. A significant positive cluster ($p<0.05$) can be seen in right-hemispheric regions. (**C**) Maxima of source level differences for the comparison of congruent and incongruent pairs of stimuli (tested two-sided with only positive, uncorrected t-values above the 95th percentile shown; see Table 2B for MNI coordinates of maxima).

For the late theta-band window (750 to 1250 ms), source estimation revealed activity patterns to be enhanced compared to baseline in prefrontal and inferior temporal regions. Source differences between congruent and incongruent pairs of visual-tactile stimulus pairs were found in right-hemispheric supramarginal gyrus with higher power values being associated with congruent stimulus pairs (see Table 2B for the corresponding MNI coordinates). Figure 5C shows the source power contrast for late theta-band responses in the *congruence evaluation task* in uncorrected t-values.

3.2.3 Comparison between detection and congruence evaluation task

To investigate global inter-task differences in neuronal activity associated with distinct cognitive demands, we compared alpha- and beta-band specific responses (raw power values) for the *detection* and the *congruence evaluation task* in an interval directly preceding stimulus presentation (– 250 ms to 0). Data were averaged across conditions within the two tasks and thereafter compared between the tasks. Significant differences in pre-stimulus activity were found for both frequency ranges. Employing a cluster level randomization approach, we found pre-stimulus alpha-band power (8 to 13 Hz) to be reduced for the *detection task* as

compared to the *congruence evaluation* task, resulting in a negative cluster ($p < 0.01$) apparent in right-hemispheric central regions and a second one in left posterior scalp locations ($p < 0.05$, Figure 6A).

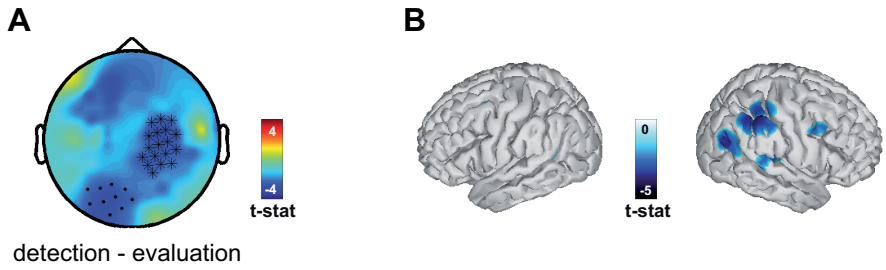

Figure 6. Comparison of alpha-band pre-stimulus activity between the *detection* and the *congruence evaluation task*. (**A**) Topography of the differences (shown in t-values) in alpha-band power (8-13 Hz) in a time interval from – 250 ms to 0 (onset of the visual and tactile stimuli). A significant negative cluster ($p<0.01$) is apparent in right-central scalp regions. A second cluster at left-posterior locations is significant with $p<0.05$. (**B**) Maxima of source level differences for the comparison of anticipatory alpha-band power between the two tasks (tested two-sided with only negative, uncorrected t-values below the fifth percentile displayed here). For MNI coordinates of maxima see Table 2C.

Pre-stimulus alpha-band power was maximal in higher visual areas (V3) for both tasks. Differences in anticipatory alpha-band activity were mainly located in posterior cingulate cortex, right-hemispheric superior temporal and supramarginal gyrus (Figure 6B; see Table 2C for MNI coordinates of maximal differences).

Contrasting pre-stimulus beta-band responses (13 to 25 Hz) between the two tasks also resulted in a negative cluster ($p < 0.01$), the spatial distribution being more extended and slightly more central (Figure 7A). Also in the beta-frequency range, anticipatory neuronal activity was more pronounced for the *congruence evaluation task*.

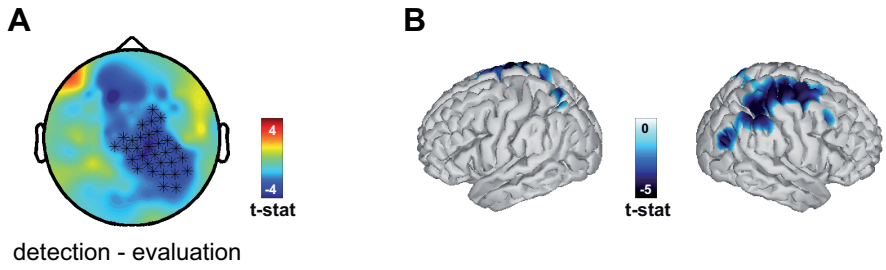

Figure 7. Comparison of beta-band pre-stimulus activity between the *detection* and the *congruence evaluation task*. (**A**) Topography of the differences (shown in t-values) in beta-band power (13-25 Hz) in a time interval from – 250 ms to 0 (onset of the visual and tactile stimuli). A significant negative cluster ($p<0.01$) spanning from central to right lateral regions is apparent. (**B**) Maxima of source level differences for the comparison of anticipatory beta-band power between the two tasks (tested two-sided with only negative, uncorrected t-values below the fifth percentile displayed here). For MNI coordinates of maxima see Table 2C.

Pre-stimulus beta-band activity was maximal in visual cortex (V2 and V3) and in inferior temporal gyrus. Contrasting pre-stimulus beta-band activity between the two tasks yielded maximal differences in right angular gyrus, supramarginal gyrus and bihemispheric somatosensory association cortex (Figure 7B).

In a second step, we checked for differences in frequency-specific responses related to task demands by comparing responses to congruent VT targets of the *detection task* and matching stimulus pairs of the *congruence evaluation task* (two conditions employing identical physical stimulation) within the time-frequency windows of interest. The windows chosen for our analysis are reported in the Methods section (see also Figure 2A and 2B). Again, we report on statistically significant comparisons only.

Descriptively, theta-band power in a time window from 0 to 750 ms was augmented as compared to baseline level across the whole scalp, with the maxima being located at fronto-central, right-lateral and right-posterior locations for both, congruent VT targets of the *detection tas*k and matching stimulus pairs of the *congruence evaluation* (see Figure 8A). Comparing theta-band power between these conditions yielded significant differences. Theta-

band responses were more pronounced for congruent VT targets in fronto-central and right-posterior regions (the corresponding cluster was significant with $p < 0.01$, Figure 8B).

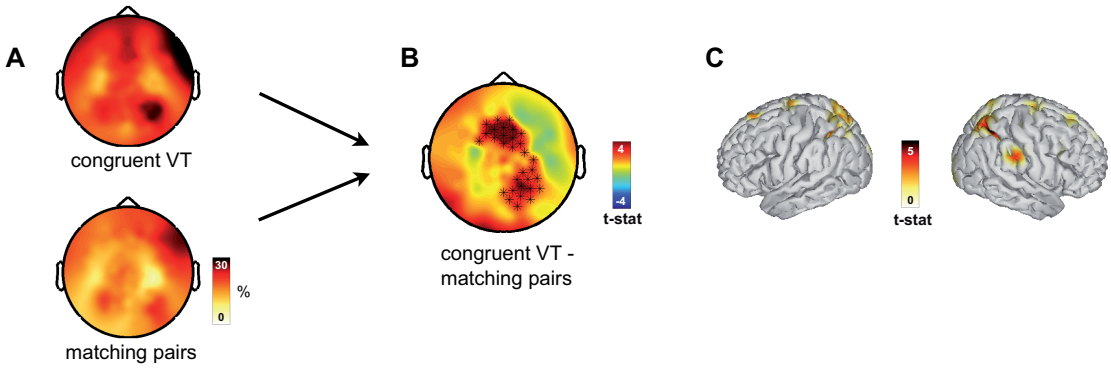

Figure 8. Comparison of theta-band responses between the *detection* and the *congruence evaluation task*. (**A**) Power for theta-band frequencies (2-7 Hz) for congruent VT targets of the *detection task* and matching pairs of the *congruence evaluation task* in a time window from 0 to 750 ms after stimulation, expressed as relative change to baseline (in %). (**B**) Topography of the differences (shown in t-values) in theta-band power. A significant positive cluster ($p<0.01$) can be seen in fronto-central and right-posterior scalp locations. (**C**) Maxima of source level differences for the comparison of congruent VT targets and matching visual-tactile pairs shown in uncorrected t-values (tested two-sided with only positive, uncorrected t-values above the 95th percentile displayed here; see Table 2C for MNI coordinates of maxima).

For theta-band responses to congruent VT targets of the *detection task* and congruent stimulus pairs of the *congruence evaluation task* between stimulus onset and 750 ms, source estimation revealed maxima for both conditions to be located in anterior cingulate cortex. Task-related differences in theta-band responses to crossmodally congruent stimulus combinations were mainly found in right somatosensory association cortex, retrosplenial cingulate cortex and supramarginal gyrus (Figure 8C).

Table 2. MNI coordinates and uncorrected t-values of the voxels showing maximal statistical difference between conditions respectively tasks. Results are shown for source estimates of frequency-band specific condition differences within the *detection* and the *congruence evaluation task*, as well as the comparison between the two tasks.

A *Detection task*

Region	**X**	**Y**	**Z**	**t-value**
Alpha-band responses for congruent VT vs. incongruent V targets (250-750 ms)				
Prefrontal cortex (right)	44	51	– 4	– 6.9
Supramarginal gyrus (left)	– 64	– 49	35	– 3.9
Alpha-band responses for congruent VT vs. incongruent T targets (250-750 ms)				
Premotor cortex (right)	43	– 19	65	– 4.3
Supramarginal gyrus (right)	58	– 45	25	– 3.9
Somatosensory association cortex (right)	6	– 69	63	– 3.8
Superior frontal gyrus (right)	24	58	32	– 3.5
Beta-band responses for congruent VT vs. incongruent V targets (750-1250 ms)				
Somatosensory association cortex (right)	29	– 39	51	5.2
Premotor cortex (right)	57	5	46	3.7
Beta-band responses for congruent VT vs. incongruent T targets (750-1250 ms)				
Prefrontal cortex (left)	– 8	73	11	5.8
Premotor cortex (right)	18	– 28	77	4
Somatosensory association cortex (left)	–13	– 50	79	3.6
Premotor cortex (left)	–56	4	48	3.1

B *Congruence evaluation task*

Region	**X**	**Y**	**Z**	**t-value**
Theta-band responses for matching vs. non-matching stimulus pairs (750-1250 ms)				
Supramarginal gyrus (right)	31	– 47	44	3.8

C *Comparison between detection task and congruence evaluation task*

Region	**X**	**Y**	**Z**	**t-value**
Pre-stimulus alpha-band responses for detection vs. congruence evaluation task (– 250-0 ms*)*				
Posterior cingulate cortex (left)	– 18	– 58	10	– 3.3
Superior temporal gyrus (right)	61	– 42	13	– 3.3
Supramarginal gyrus (right)	43	– 46	66	– 3.1
Pre-stimulus beta-band responses for detection vs. congruence evaluation task (– 250-0 ms*)*				
Angular gyrus (right)	43	– 79	33	– 4.4
Supramarginal gyrus (right)	44	– 48	56	– 3.8
Somatosensory association cortex (left)	– 18	– 66	68	– 3.8
Somatosensory association cortex (right)	37	– 58	64	– 3.6
Theta-band responses for congruent VT targets vs. matching pairs (0-750 ms)				
Somatosensory association cortex (right)	25	– 60	58	5.9
Retrosplenial cingulate cortex (right)	5	– 41	39	5.1
Supramarginal gyrus (right)	63	– 34	41	4.3

4. Discussion

In the present study we investigated behavioral and oscillatory signatures of visual-tactile stimulus congruence effects by means of a crossmodal pattern matching paradigm involving two different tasks. On a behavioral level, we found evidence for stimulus-congruence related enhancement in performance, replicating our previous findings (Göschl et al., 2014). Within the *detection* and the *congruence evaluation task*, differences in oscillatory dynamics associated with pattern congruence were manifold and involved theta- (2-7 Hz), alpha- (8-13 Hz) and beta-band (13-25 Hz) frequencies, possibly pertaining to different subcomponents of multisensory integration.

Comparing the *detection* and the *congruence evaluation task*, differences in anticipatory neuronal activity were apparent in alpha- and beta-frequency ranges showing power values to be less pronounced for the *detection task*. Additionally, task-related differences were represented in theta-band power, showing stronger modulation in an early time window for congruent stimulus pairs of the *detection task* as compared to matching pairs of the *congruence evaluation task*.

In the following, we discuss stimulus congruence-related as well as task-related effects in our visual-tactile matching paradigm in detail.

4.1 Detection task

Using stimulus material comparable to our study, the relevance of oscillatory brain activity in mediating multisensory interactions has been shown before (Bauer et al., 2009; Bauer et al., 2012; Kanayama and Ohira, 2009; Kanayama et al., 2012). Here, we add to the existing literature by showing that the crossmodal relation of stimuli presented in two sensory modalities is critical for performance and that congruence-related behavioral gains are

mediated by low frequency oscillatory activity. For the simultaneous detection of visual and tactile targets, we find alpha-band decreases to be more pronounced for congruent targets as compared to either incongruent target case. We suggest that this is indicative of strengthened bottom-up stimulus processing related to crossmodal congruence. It has been proposed recently that information transfer in the human brain is organized by inhibiting task-irrelevant regions and that this functional inhibition is reflected in oscillatory activity in the alpha-band ("gating by inhibition", Jensen and Mazaheri, 2010; Jensen et al., 2014). In the current study, alpha-band decreases found to be more prominent for congruent targets might be due to an enhanced release from inhibition, mainly apparent in right central and left posterior scalp areas. Using a navigation paradigm to investigate integration of vestibular and kinesthetic information, alpha suppression in occipital, parietal and temporal clusters was strongest in incongruent conditions, when different sensory modalities did not match (Ehinger et al. 2014). In that paradigm incongruent trials led to conflicting information, which should be integrated by default. In the current task, however, targets had to be detected in either modality, which is equivalent to a logical OR, and incongruent trials still had a well-defined required response. Thus, given the proposed ties of alpha-band activity and attentional processes (Jensen and Mazaheri, 2010; Klimesch, 2012; Palva and Palva, 2007), the stronger alpha-band suppression found here might also be due to more attentional capture of congruent stimulus pairs and subsequently lead to enhanced processing. Source estimation revealed maxima for alpha-band differences to be located in prefrontal areas and parietal cortex (supramarginal gyrus and somatosensory association cortex) which might point to enhanced processing for congruent stimulus combinations in areas linked to multisensory integration (Calvert, 2001; Ghazanfar and Schroeder, 2006).

Beta-band activity in a time interval directly preceding participants' response on the task differed significantly between congruent and incongruent visual-tactile stimulus pairs. There is evidence that beta-band activity is related to multisensory processing (e.g. Senkowski et al.,

2006; Schepers et al., 2013) but its role in mediating crossmodal congruence effects is unclear. Differences in late beta-band power found in the current experiment show maxima in prefrontal areas, premotor and somatosensory association cortex. Therefore, we hypothesize that processes of perceptual decision making may be reflected in these activation differences. Recent work by Donner and colleagues (2007, 2009) has linked beta-band activity to choice behavior in a visual motion detection task and stated that performance-predictive activity is expressed in posterior parietal and prefrontal cortices. Given the match of differences in behavioral performance for congruent VT targets, incongruent V and incongruent T targets and late beta-band power for the different conditions, we speculate that beta-band power is linked to decision making also in the current study. In this sense, congruent visual-tactile stimulus pairs as compared to either incongruent target case might be viewed as stronger sensory evidence for an upcoming decision and the corresponding motor response (press the 'target' button). This choice-related activity could be reflected in beta-band power (Donner et al., 2007; Donner et al., 2009).

4.2 Congruence evaluation task

Within the *congruence evaluation task*, differences in oscillatory dynamics between matching and non-matching visual-tactile pairs were restricted to late responses in the theta-range. In general, the modulation of theta-frequencies in the integration of features across sensory modalities is in agreement with previous reports (van Ackeren et al., 2014). For the comparison of congruent and incongruent stimulation, theta-band power has been shown to be more pronounced for the incongruent case which in turn has been linked to processes of conflict monitoring and conflict resolution, respectively (Cohen and Donner, 2013; Cohen and Ridderinkhof, 2013; Kanayama and Ohira, 2009). Here, we find theta-band power to be stronger for congruent stimulus pairs and this effect is located in supramarginal gyrus, an area of secondary somatosensory representation linked to a broad range of cognitive functions,

including texture and pattern discrimination (e.g. Hegner et al., 2010). Given the differences in the definition of congruence between our study and related work (where congruence mostly refers to spatial proximity) and the temporal structure of the observed effects, we suggest that power increases found here may reflect inter-sensory facilitation effects in pattern discrimination resulting from visual-tactile congruence. Nevertheless, one might speculate that the centrally distributed negative cluster (though not reaching statistical significance) apparent in Figure 5B relates to processes of conflict monitoring associated with response selection.

4.3 Comparison between detection and congruence evaluation task

Direct comparison of neuronal activity between the *detection* and the *congruence evaluation task* was limited by the different designs of the two tasks, which is why we focused on pre-stimulus activity contrasts on the one hand and a comparison of oscillatory signatures between congruent pairs of stimuli for the *detection* and the *congruence evaluation task* on the other hand.

As suggested by the concept of functional inhibition by alpha-oscillations (Jensen and Mazaheri, 2010; Jensen et al., 2014; see also Klimesch et al., 2007), we hypothesized that differences in cognitive demands imposed by the two tasks would modulate preparatory oscillatory activity differentially in alpha-/beta-frequencies (see also Mazaheri et al., 2014). Contrasting alpha-band activity before stimulus onset for *detection* versus *congruence evaluation* indeed yielded significant differences showing a power decrease in right-central scalp locations. At the source level, maxima of these differences were located in posterior cingulate cortex, superior temporal and supramarginal gyrus. Interpreted in the context of multisensory perceptual gating this finding could point to a higher contribution of areas related to multisensory processing (mainly the superior temporal gyrus; see Doermann and Naumer, 2005; Ghazanfar and Schroeder, 2006) for the *detection task*. Alternatively, but

within the same framework of gating by inhibition, one could argue that the task difference found here reflects processes related to working memory. The posterior cingulate cortex has been linked to memory processes (Nielsen et al., 2005) and decreases in this area found in our study possibly relate to either the maintenance of the target pattern in working memory or preparatory activity for memory matching that are specific for the *detection task*.

Similarly, differences in beta-band power before stimulus onset between *detection* and *congruence evaluation task* were mapped to a negative cluster in mainly right-hemispheric regions. The spatial distribution was somewhat more extended, additionally containing regions of angular gyrus and somatosensory association cortex. Again, decreased activity could be interpreted in terms of higher engagement of these regions in the *detection task*. Comparing the involvement of somatosensory association cortex between the tasks, we propose that beta-band decreases for the *detection task* could also signal preparatory processes of motor decision making. For the *congruence evaluation task*, these processes might be delayed due to additional processing effort linked to explicitly evaluating the relation between the visual and the tactile pattern. Support for this idea can be found in our previous study (Göschl et al., 2014) reporting larger response latencies for the *congruence evaluation task*.

The interpretation of pre-stimulus differences in oscillatory alpha-band activity in the context of working memory function is also compatible with the finding of increased theta-band power in response to congruent visual-tactile stimulus pairs of the *detection task* as compared to matching pairs of the *congruence evaluation task*. We propose that theta-band modulations are indicative of working memory processes (concordant with recent work, see for example Benchenane et al., 2011; Hsieh and Ranganath, 2014; Sauseng et al., 2010), which are more relevant in the target *detection* than the *congruence evaluation* task. Beside somatosensory association cortex and supramarginal gyrus, source estimation revealed difference maxima in retrosplenial cortex, a region implicated in memory function (Vann et al., 2009), which supports this interpretation.

Source reconstruction showed prominent involvement of parietal and superior temporal cortex – brain regions traditionally implicated in multisensory integration – for both tasks of the current study. Interestingly, we found evidence for more engagement of these regions in the *detection* rather than the *congruence evaluation task*. Whereas stimulus congruence only implicitly plays a role in the former task, the latter demands to explicitly evaluate the crossmodal relation of the two stimuli. Future work needs to further determine the relation of task demands and bottom-up stimulus congruence and their reflection in neuronal oscillations. The lateralized stimulus setup realized in the current experiment permits to study inter-hemispheric synchronization as a measure for multimodal interactions. The question whether the observed cortical activations result from lateralized stimulation or rather from cortical asymmetry goes beyond the scope of the current work and remains to be clarified in future studies. However, the pronounced involvement of right-hemispheric cortical regions for the spatial pattern matching task used here is well compatible with experimental evidence on a dominant role of the right hemisphere in spatial processing (see for example Hegner et al., 2010).

4.4 Conclusions

The current study adds to increasing evidence that neuronal oscillations are involved in multisensory interactions. Specifically, oscillatory activity in lower frequency ranges (below 30 Hz) seems to be able to mediate long-range communication that is crucial for crossmodal processing. Here we studied visual-tactile interactions as a model for integration in distributed networks und found differences in oscillatory dynamics related to crossmodal congruence in theta-, alpha- and beta-frequency ranges. We propose that these differences relate to distinct subcomponents of multisensory integration, for instance processes of attentional capture, multisensory gating and perceptual decision making.

5. Acknowledgments

This research was supported by grants from the German Research Foundation (SFB 936/A3/B6) and the European Union (ERC-2010-AdG-269716) awarded to A.K.E. and P.K. The authors thank Julia Diestel for assistance in data recording, Till Schneider for helpful discussions on previous versions of the manuscript and Guido Nolte as well as Arne Ewald for methodological counseling.

6. References

Barutchu, A., Freestone, D. R., Innes-Brown, H., Crewther, D. P., & Crewther, S. G. (2013). Evidence for Enhanced Multisensory Facilitation with Stimulus Relevance: An Electrophysiological Investigation. *PLoS One*, *8*(1). doi:10.1371/journal.pone.0052978

Bauer, M., Kennett, S., & Driver, J. (2012). Attentional selection of location and modality in vision and touch modulates low-frequency activity in associated sensory cortices. *Journal of Neurophysiology*, *107*(9), 2342–2351. doi:10.1152/jn.00973.2011

Bauer, M., Oostenveld, R., & Fries, P. (2009). Tactile stimulation accelerates behavioral responses to visual stimuli through enhancement of occipital gamma-band activity. *Vision Research*, *49*(9), 931–942. doi:10.1016/j.visres.2009.03.014

Benchenane, K., Tiesinga, P. H., & Battaglia, F. P. (2011). Oscillations in the prefrontal cortex: a gateway to memory and attention. *Current Opinion in Neurobiology*, *21*(3), 475–485. doi:10.1016/j.conb.2011.01.004

Calvert, G. A. (2001). Crossmodal Processing in the Human Brain: Insights from Functional Neuroimaging Studies. *Cerebral Cortex*, *11*(12), 1110–1123. doi:10.1093/cercor/11.12.1110

Cohen, M. X. (2014). *Analyzing Neural Time Series Data: Theory and Practice*. MIT Press.

Cohen, M. X., & Donner, T. H. (2013). Midfrontal conflict-related theta-band power reflects neural oscillations that predict behavior. *Journal of Neurophysiology*, *110*(12), 2752–2763. doi:10.1152/jn.00479.2013

Cohen, M. X., & Ridderinkhof, K. R. (2013). EEG source reconstruction reveals frontal-parietal dynamics of spatial conflict processing. *PLoS One*, *8*(2), e57293. doi:10.1371/journal.pone.0057293

Delorme, A., & Makeig, S. (2004). EEGLAB: an open source toolbox for analysis of single-trial EEG dynamics including independent component analysis. *Journal of Neuroscience Methods*, *134*(1), 9–21. doi:10.1016/j.jneumeth.2003.10.009

Diederich, A., & Colonius, H. (2007). Modeling spatial effects in visual-tactile saccadic reaction time. *Perception & Psychophysics*, *69*(1), 56–67.

Doehrmann, O., & Naumer, M. J. (2008). Semantics and the multisensory brain: How meaning modulates processes of audio-visual integration. *Brain Research*, *1242*, 136–150. doi:10.1016/j.brainres.2008.03.071

Doesburg, S. M., Emberson, L. L., Rahi, A., Cameron, D., & Ward, L. M. (2008). Asynchrony from synchrony: long-range gamma-band neural synchrony accompanies perception of audiovisual speech asynchrony. *Experimental Brain Research*, *185*(1), 11–20. doi:10.1007/s00221-007-1127-5

Doesburg, S. M., Green, J. J., McDonald, J. J., & Ward, L. M. (2009). From local inhibition to long-range integration: A functional dissociation of alpha-band synchronization across cortical scales in visuospatial attention. *Brain Research*, *1303*, 97–110. doi:10.1016/j.brainres.2009.09.069

Donner, T. H., & Siegel, M. (2011). A framework for local cortical oscillation patterns. *Trends in Cognitive Sciences*, *15*(5), 191–199. doi:10.1016/j.tics.2011.03.007

Donner, T. H., Siegel, M., Fries, P., & Engel, A. K. (2009). Buildup of Choice-Predictive Activity in Human Motor Cortex during Perceptual Decision Making. *Current Biology*, *19*(18), 1581–1585. doi:10.1016/j.cub.2009.07.066

Donner, T. H., Siegel, M., Oostenveld, R., Fries, P., Bauer, M., & Engel, A. K. (2007). Population Activity in the Human Dorsal Pathway Predicts the Accuracy of Visual Motion Detection. *Journal of Neurophysiology*, *98*(1), 345–359. doi:10.1152/jn.01141.2006

Driver, J., & Spence, C. (2000). Multisensory perception: beyond modularity and convergence. *Current Biology: CB*, *10*(20), R731–735.

Ehinger, B.V., Fischer, P., Gert, A.L., Kaufhold, L., Weber, F., Pipa, G., & König, P. (2014). Kinesthetic and vestibular information modulate alpha activity during spatial navigation: A mobile EEG study. *Frontiers in Human Neuroscience*, 8: 71. doi: 10.3389/fnhum.2014.00071

Engel, A. K., Fries, P., & Singer, W. (2001). Dynamic predictions: Oscillations and synchrony in top-down processing. *Nature Reviews Neuroscience*, *2*(10), 704–716. doi:10.1038/35094565

Forster, B., Cavina-Pratesi, C., Aglioti, S. M., & Berlucchi, G. (2002). Redundant target effect and intersensory facilitation from visual-tactile interactions in simple reaction time. *Experimental Brain Research*, *143*(4), 480–487. doi:10.1007/s00221-002-1017-9

Frassinetti, F., Bolognini, N., & Làdavas, E. (2002). Enhancement of visual perception by crossmodal visuo-auditory interaction. *Experimental Brain Research*, *147*(3), 332–343. doi:10.1007/s00221-002-1262-y

Friese, U., Köster, M., Hassler, U., Martens, U., Trujillo-Barreto, N., & Gruber, T. (2013). Successful memory encoding is associated with increased cross-frequency coupling between frontal theta and posterior gamma oscillations in human scalp-recorded EEG. *NeuroImage*, *66*, 642–647. doi:10.1016/j.neuroimage.2012.11.002

Ghazanfar, A. A., & Schroeder, C. E. (2006). Is neocortex essentially multisensory? *Trends in Cognitive Sciences*, *10*(6), 278–285. doi:10.1016/j.tics.2006.04.008

Gillmeister, H., & Eimer, M. (2007). Tactile enhancement of auditory detection and perceived loudness. *Brain Research*, *1160*, 58–68. doi:10.1016/j.brainres.2007.03.041

Gleiss, S., & Kayser, C. (2014a). Oscillatory mechanisms underlying the enhancement of visual motion perception by multisensory congruency. *Neuropsychologia*. doi:10.1016/j.neuropsychologia.2013.11.005

Gleiss, S., & Kayser, C. (2014b). Acoustic Noise Improves Visual Perception and Modulates Occipital Oscillatory States. *Journal of Cognitive Neuroscience*, *26*(4), 699–711. doi:10.1162/jocn_a_00524

Göschl, F., Engel, A. K., & Friese, U. (2014). Attention modulates visual-tactile interaction in spatial pattern matching. *PLoS One*, *9*(9), e106896. doi:10.1371/journal.pone.0106896

Hassler, U., Friese, U., Martens, U., Trujillo-Barreto, N., & Gruber, T. (2013). Repetition priming effects dissociate between miniature eye movements and induced gamma-band responses in the human electroencephalogram. *European Journal of Neuroscience*, *38*(3), 2425–2433. doi:10.1111/ejn.12244

Hassler, U., Trujillo Barreto, N., & Gruber, T. (2011). Induced gamma band responses in human EEG after the control of miniature saccadic artifacts. *NeuroImage*, *57*(4), 1411–1421. doi:10.1016/j.neuroimage.2011.05.062

Hegner, Y. L., Lee, Y., Grodd, W., & Braun, C. (2010). Comparing Tactile Pattern and Vibrotactile Frequency Discrimination: A Human fMRI Study. *Journal of Neurophysiology*, *103*(6), 3115–3122. doi:10.1152/jn.00940.2009

Hipp, J. F., Engel, A. K., & Siegel, M. (2011). Oscillatory Synchronization in Large-Scale Cortical Networks Predicts Perception. *Neuron*, *69*(2), 387–396. doi:10.1016/j.neuron.2010.12.027

Hsieh, L.-T., & Ranganath, C. (2014). Frontal midline theta oscillations during working memory maintenance and episodic encoding and retrieval. *NeuroImage*, *85, Part 2*, 721–729. doi:10.1016/j.neuroimage.2013.08.003

Hummel, F., & Gerloff, C. (2005). Larger Interregional Synchrony is Associated with Greater Behavioral Success in a Complex Sensory Integration Task in Humans. *Cerebral Cortex*, *15*(5), 670–678. doi:10.1093/cercor/bhh170

Jensen, O., & Mazaheri, A. (2010). Shaping functional architecture by oscillatory alpha activity: gating by inhibition. *Frontiers in Human Neuroscience*, *4*, 186. doi:10.3389/fnhum.2010.00186

Jensen, O., Gips, B., Bergmann, T. O., & Bonnefond, M. (2014). Temporal coding organized by coupled alpha and gamma oscillations prioritize visual processing. *Trends in Neurosciences*, *37*(7), 357–369. doi:10.1016/j.tins.2014.04.001

Jokisch, D., & Jensen, O. (2007). Modulation of Gamma and Alpha Activity during a Working Memory Task Engaging the Dorsal or Ventral Stream. *The Journal of Neuroscience*, *27*(12), 3244–3251. doi:10.1523/JNEUROSCI.5399-06.2007

Kalcher, J., & Pfurtscheller, G. (1995). Discrimination between phase-locked and non-phase-locked event-related EEG activity. *Electroencephalography and Clinical Neurophysiology*, *94*(5), 381–384.

Kanayama, N., & Ohira, H. (2009). Multisensory processing and neural oscillatory responses: separation of visuotactile congruency effect and corresponding electroencephalogram activities. *Neuroreport*, *20*(3), 289–293. doi:10.1097/WNR.0b013e328322ca63

Kanayama, N., Tamè, L., Ohira, H., & Pavani, F. (2012). Top down influence on visuo-tactile interaction modulates neural oscillatory responses. *NeuroImage*, *59*(4), 3406–3417. doi:10.1016/j.neuroimage.2011.11.076

Kayser, C., Petkov, C. I., & Logothetis, N. K. (2008). Visual Modulation of Neurons in Auditory Cortex. *Cerebral Cortex*, *18*(7), 1560–1574. doi:10.1093/cercor/bhm187

Klimesch, W. (2012). Alpha-band oscillations, attention, and controlled access to stored information. *Trends in Cognitive Sciences*, *16*(12), 606–617. doi:10.1016/j.tics.2012.10.007

Klimesch, W., Sauseng, P., & Hanslmayr, S. (2007). EEG alpha oscillations: The inhibition–timing hypothesis. *Brain Research Reviews*, *53*(1), 63–88. doi:10.1016/j.brainresrev.2006.06.003

Lakatos, P., Chen, C. M., O'Connell, M. N., Mills, A., & Schroeder, C. E. (2007). Neuronal Oscillations and Multisensory Interaction in Primary Auditory Cortex. *Neuron*, *53*(2), 279–292. doi:10.1016/j.neuron.2006.12.011

Macaluso, E., & Driver, J. (2005). Multisensory spatial interactions: a window onto functional integration in the human brain. *Trends in Neurosciences*, *28*(5), 264–271. doi:10.1016/j.tins.2005.03.008

Maris, E., & Oostenveld, R. (2007). Nonparametric statistical testing of EEG- and MEG-data. *Journal of Neuroscience Methods*, *164*(1), 177–190. doi:10.1016/j.jneumeth.2007.03.024

Mazaheri, A., van Schouwenburg, M. R., Dimitrijevic, A., Denys, D., Cools, R., & Jensen, O. (2014). Region-specific modulations in oscillatory alpha activity serve to facilitate processing in the visual and auditory modalities. *NeuroImage*, *87*, 356–362. doi:10.1016/j.neuroimage.2013.10.052

McDonald, J. J., Teder-Sälejärvi, W. A., & Hillyard, S. A. (2000). Involuntary orienting to sound improves visual perception. *Nature*, *407*(6806), 906–908. doi:10.1038/35038085

McGurk, H., & MacDonald, J. (1976). Hearing lips and seeing voices. *Nature*, *264*(5588), 746–748.

Molholm, S., Ritter, W., Javitt, D. C., & Foxe, J. J. (2004). Multisensory Visual–Auditory Object Recognition in Humans: a High-density Electrical Mapping Study. *Cerebral Cortex*, *14*(4), 452–465. doi:10.1093/cercor/bhh007

Murray, M. M., Foxe, J. J., Higgins, B. A., Javitt, D. C., & Schroeder, C. E. (2001). Visuo-spatial neural response interactions in early cortical processing during a simple reaction time task: a high-density electrical mapping study. *Neuropsychologia*, *39*(8), 828–844. doi:10.1016/S0028-3932(01)00004-5

Nielsen, F. Å., Balslev, D., & Hansen, L. K. (2005). Mining the posterior cingulate: Segregation between memory and pain components. *NeuroImage*, *27*(3), 520–532. doi:10.1016/j.neuroimage.2005.04.034

Nieuwenhuis, I. L. C., Takashima, A., Oostenveld, R., Fernández, G., & Jensen, O. (2008). Visual areas become less engaged in associative recall following memory stabilization. *NeuroImage*, *40*(3), 1319–1327. doi:10.1016/j.neuroimage.2007.12.052

Nolte, G., & Dassios, G. (2005). Analytic expansion of the EEG lead field for realistic volume conductors. *Physics in Medicine and Biology*, *50*(16), 3807–3823. doi:10.1088/0031-9155/50/16/010

Oostenveld, R., Fries, P., Maris, E., & Schoffelen, J.-M. (2011). FieldTrip: Open Source Software for Advanced Analysis of MEG, EEG, and Invasive Electrophysiological Data. *Computational Intelligence and Neuroscience*, *2011*. doi:10.1155/2011/156869

Palva, S., & Palva, J. M. (2007). New vistas for α-frequency band oscillations. *Trends in Neurosciences*, *30*(4), 150–158. doi:10.1016/j.tins.2007.02.001

Pascual-Marqui, R.D., 2007. Discrete, 3D distributed, linear imaging methods of electric neuronal activity. Part 1: Exact, Zero Error Localization, (arXiv:0710.3341 [math-ph], October 17, available: http://arxiv.org/abs/0710.3341)

Sauseng, P., Griesmayr, B., Freunberger, R., & Klimesch, W. (2010). Control mechanisms in working memory: A possible function of EEG theta oscillations. *Neuroscience & Biobehavioral Reviews*, *34*(7), 1015–1022. doi:10.1016/j.neubiorev.2009.12.006

Schepers, I. M., Schneider, T. R., Hipp, J. F., Engel, A. K., & Senkowski, D. (2013). Noise alters beta-band activity in superior temporal cortex during audiovisual speech processing. *NeuroImage*, *70*, 101–112. doi:10.1016/j.neuroimage.2012.11.066

Schneider, T. R., Engel, A. K., & Debener, S. (2008). Multisensory identification of natural objects in a two-way crossmodal priming paradigm. *Experimental Psychology*, *55*(2), 121–132.

Schneider, T. R., Lorenz, S., Senkowski, D., & Engel, A. K. (2011). Gamma-Band Activity as a Signature for Cross-Modal Priming of Auditory Object Recognition by Active Haptic Exploration. *The Journal of Neuroscience*, *31*(7), 2502–2510. doi:10.1523/JNEUROSCI.6447-09.2011

Senkowski, D., Molholm, S., Gomez-Ramirez, M., & Foxe, J. J. (2006). Oscillatory Beta Activity Predicts Response Speed during a Multisensory Audiovisual Reaction Time Task: A High-Density Electrical Mapping Study. *Cerebral Cortex*, *16*(11), 1556–1565. doi:10.1093/cercor/bhj091

Senkowski, D., Schneider, T. R., Foxe, J. J., & Engel, A. K. (2008). Crossmodal binding through neural coherence: implications for multisensory processing. *Trends in Neurosciences*, *31*(8), 401–409. doi:10.1016/j.tins.2008.05.002

Singer, W., & Gray, C. M. (1995). Visual Feature Integration and the Temporal Correlation Hypothesis. *Annual Review of Neuroscience*, *18*(1), 555–586. doi:10.1146/annurev.ne.18.030195.003011

Singh, A. K., Okamoto, M., Dan, H., Jurcak, V., & Dan, I. (2005). Spatial registration of multichannel multi-subject fNIRS data to MNI space without MRI. *NeuroImage*, *27*(4), 842–851. doi:10.1016/j.neuroimage.2005.05.019

Stein, B. E. (2012). *The New Handbook of Multisensory Processing*. Mit Press.

Van Ackeren, M. J., Schneider, T. R., Müsch, K., & Rueschemeyer, S.-A. (2014). Oscillatory Neuronal Activity Reflects Lexical-Semantic Feature Integration within and across Sensory Modalities in Distributed Cortical Networks. *The Journal of Neuroscience*, *34*(43), 14318–14323. doi:10.1523/JNEUROSCI.0958-14.2014

Van Driel, J., Knapen, T., van Es, D. M., & Cohen, M. X. (2014). Interregional alpha-band synchrony supports temporal cross-modal integration. *NeuroImage*, *101*, 404–415. doi:10.1016/j.neuroimage.2014.07.022

Van Ede, F, Lange, F. de, Jensen, O., & Maris, E. (2011). Orienting Attention to an Upcoming Tactile Event Involves a Spatially and Temporally Specific Modulation of Sensorimotor Alpha- and Beta-Band Oscillations. *The Journal of Neuroscience*, *31*(6), 2016–2024. doi:10.1523/JNEUROSCI.5630-10.2011

Van Ede, F., Szebényi, S., & Maris, E. (2014). Attentional modulations of somatosensory alpha, beta and gamma oscillations dissociate between anticipation and stimulus processing. *NeuroImage*, *97*, 134–141. doi:10.1016/j.neuroimage.2014.04.047

Vann, S. D., Aggleton, J. P., & Maguire, E. A. (2009). What does the retrosplenial cortex do? *Nature Reviews Neuroscience*, *10*(11), 792–802. doi:10.1038/nrn2733

Varela, F., Lachaux, J.-P., Rodriguez, E., & Martinerie, J. (2001). The brainweb: Phase synchronization and large-scale integration. *Nature Reviews Neuroscience*, *2*(4), 229–239. doi:10.1038/35067550

Von Stein, A., Chiang, C., & König, P. (2000). Top-down processing mediated by inter-areal synchronization. *Proc Natl Acad Sci USA,* 97, 14748-14753. doi:10.1073/pnas.97.26.14748

Womelsdorf, T., Schoffelen, J.-M., Oostenveld, R., Singer, W., Desimone, R., Engel, A. K., & Fries, P. (2007). Modulation of Neuronal Interactions Through Neuronal Synchronization. *Science*, *316*(5831), 1609–1612. doi:10.1126/science.1139597